# Periodicity of a fast radio burst explained by transits of Trojan and Hildas asteroids orbiting a pulsar

Guillaume Voisin, Fabrice Mottez, Philippe Zarka

▶ **To cite this version:**

Guillaume Voisin, Fabrice Mottez, Philippe Zarka. Periodicity of a fast radio burst explained by transits of Trojan and Hildas asteroids orbiting a pulsar. 2020. hal-02862813v1

**HAL Id: hal-02862813**

**https://hal.science/hal-02862813v1**

Preprint submitted on 9 Jun 2020 (v1), last revised 21 Sep 2021 (v2)

**HAL** is a multi-disciplinary open access archive for the deposit and dissemination of scientific research documents, whether they are published or not. The documents may come from teaching and research institutions in France or abroad, or from public or private research centers.

L'archive ouverte pluridisciplinaire **HAL**, est destinée au dépôt et à la diffusion de documents scientifiques de niveau recherche, publiés ou non, émanant des établissements d'enseignement et de recherche français ou étrangers, des laboratoires publics ou privés.

*Astronomy & Astrophysics* manuscript no. output
June 9, 2020
©ESO 2020

# Periodicity of a fast radio burst explained by transits of Trojan and Hildas asteroids orbiting a pulsar

G. Voisin[1,2,⋆], Fabrice Mottez[2], and Philippe Zarka[3]

[1] Jodrell Bank Centre for Astrophysics, School of Physics and Astronomy, The University of Manchester, M13 9PL, UK
e-mail: guillaume.voisin@manchester.ac.uk
[2] LUTh, Observatoire de Paris, PSL Research University, CNRS, Université de Paris, Sorbonne Université, 5 place Jules Janssen, 92190 Meudon, France
[3] LESIA, Observatoire de Paris, PSL Research University, CNRS, Université de Paris, Sorbonne Université, 5 place Jules Janssen, 92190 Meudon, France

Received September 15, 1996; accepted March 16, 1997

**ABSTRACT**

*Context.* Observation of fast radio bursts (FRBs) are rising very quickly with the advent of specialised instruments and surveys. Recently, it has been shown for the first time that some of them repeat quasi-periodically, with evidence of a $P = 16.35$ day period being reported in particular for FRB 180916.J0158+65.
*Aims.* We apply to FRB 180916.J0158+65 a model by which FRBs are caused by the interaction between a pulsar or magnetar wind with orbiting asteroid or planetoid-size companions forming so-called Alfven wings.
*Methods.* We use the properties of the 28 bursts collected by the CHIME/FRB collaboration over a span of 408 days in order to infer possible characteristics of asteroid swarms and pulsar wind at their origin. We perform parametric studies to explore the parameter space.
*Results.* We find a plausible configuration in which a young pulsar is orbited by a main companion with a period three times longer than apparent in the CHIME/FRB data, at $3P = 49$ days. Asteroids responsible for FRBs are located in three dynamical swarms near the L3, L4 and L5 Lagrange points akin to the Hildas class of asteroids of the Solar system. In addition, asteroids could be present in the Trojan swarms at the L4 and L5 Lagrange points. We estimate that the presence of a few thousand asteroids is necessary to produce the observed burst rate.

**Key words.** FRB: 180916.J0158+65 – (Stars:) pulsar – Minor planets, asteroids: general – Relativistic processes – Radio continuum: general

## 1. Introduction

Fast radio bursts (FRBs) consist in short, typically a few milliseconds, and intense flashes that have so far been observed only in radio bands (Petroff et al. 2019). One of their most puzzling properties is the large electron column density that the signal has crossed, the so-called dispersion measure (DM), which is encoded in their spectrum (e.g. Lyne & Graham-Smith (2012)). The measured DM is compatible with extragalactic and even cosmological distances. It is however possible that the source be in a very dense environment which would massively bias the distance estimate inferred from DM. However, a couple of FRBs, FRB 121102 (Michilli et al. 2018) and FRB 180916.J0158+65 (Marcote et al. 2020), have now been associated with host galaxies which have allowed to confirm the inferred distances and extra-galactic origin. In addition, the repetition of these two FRBs as well as a few others rules out in those cases theories appealing to cataclysmic events such as mergers or collisions. Fast radio bursts caused by Alvén wings of planets orbiting pulsars (Mottez & Zarka 2014) have been, to our knowledge, the first theory predicting a periodic repetition of FRBs. Although such perfect periodicity has so far not been observed, we believe that this theory has a few characteristics that are appealing for any theory of FRBs. Alfvén wings are akin to a plasma wake left by electrically conducting object immersed in a magnetised wind which have been originally theorised, and observed, in the context of the Jupiter-Io interaction (Neubauer 1980). These wings are favourable sites for radio-emitting plasma instabilities such as the cyclotron maser instability (Mottez & Zarka 2014). In the particular case of a pulsar the wind is ultra-relativistic with the immediate consequence that any radiation in the wing is highly collimated within a cone of aperture $\sim 1/\gamma$ where $\gamma \lesssim 10^6$ is the Lorentz factor of the wind. Thus, a few interesting characteristics follow: i) compared to isotropic emission scenarios that require tremendous amounts of energy here little is necessary to produce the observed radio flux, ii) no high-energy counterpart is expected which is in agreement with observations, iii) we know that objects orbiting pulsars are common, only is it unlikely to observe a galactic FRB due to their very a narrow beam, and iv) this very narrow beam explains the short burst duration.

We have recently shown (Mottez et al. arXiv:2002.12834 submitted to A&A, hereafter MZV20) that Alfvén wings of small bodies, such as asteroids and planetoids, can be sufficient to generate FRBs while being sufficiently far from the neutron star to survive evaporation from the intense irradiation by the pulsar and its environment. In turn, this opens the possibility of bursts occurring at seemingly random intervals if asteroids come in belts or swarms. In that latter case, one would expect groups of FRB events occurring periodically within a time win-

⋆ Secondary email: astro.guillaume.voisin@gmail.com

dow corresponding to the range of orbital phases occupied by the swarm. We call this a swarm transit. Within these swarm transits, each asteroid favourably located along the line of sight may contribute several FRBs in short, apparently random, sequences, as a result of erratic motion of the emission beam in the turbulent pulsar wind. In addition, no strict periodicity between individual event would occur due to motion within the swarm and, depending of the density of objects, some transit windows might contain no event at all. This behaviour seems to be precisely what has recently been reported concerning FRB 180916.J0158+65 (Collaboration et al. 2020). Indeed, the quasi-daily monitoring of the source by CHIME/FRB over 408 days with a daily exposure of $\sim$ 15min has resulted in the detection of 28 events which appear to be bunched in 4-day windows around a period $P = 16.35 \pm 0.18$ days. In this letter, we propose a theory based on Mottez & Zarka (2014) and MZV20 compatible with the reported observations of FRB 180916.J0158+65 . We also propose a set of predictions that will be falsifiable in the near future provided regular observations of this FRB are continued.

## 2. Trojans and Hildas-type asteroid swarms

### 2.1. Asteroids with period P

Let us assume that a swarm of asteroids orbiting a pulsar is indeed responsible for the observed bursts of FRB 180916.J0158+65 . Then, this swarm is orbiting at $P = 16.35 \pm 0.18$ days, which is the orbital period favoured by the search realised in Collaboration et al. (2020). The 4-day window then implies that the swarm covers about $1/4^{th}$ of its orbit at a distance $\sim$ 0.14AU from the neutron star (assuming a mass 1.4 times the Sun's). Such a swarm would be gravitationally unbound as can be seen from the fact that a companion with a Roche lobe covering that much of the orbit would require a body which mass would be larger than the neutron star itself. Although one could invoke the disruption of a planet due to tidal forces and/or overheating by the pulsar wind (Kotera et al. 2016), the probability of catching such an event seems unlikely. An asteroid arc following a disruption would diffuse until it forms an asteroid belt unless some very special dynamical mechanism keeps it stable. Let us note that, although unlikely, such arcs – named Liberté - Egalité - Fraternité – exist around Neptune. They are highly dynamic, and maybe unstable (Sicardy & Lissauer 1992; de Pater et al. 2005).

### 2.2. Trojans with period 3P

In the Solar system the Trojans asteroids are co-rotating with the $L_4$ and $L_5$ Lagrange points of the Sun-Jupiter system (the swarm around $L_4$ is also called the Greek camp by opposition to the Trojan camp at $L_5$). Each swarm spans $\sim 90^\circ$ of orbital phase (Levison et al. 1997) and more than $20^\circ$ in inclination [1]. In that respect, Trojan swarms accompanying what we shall call the main pulsar companion are good candidates for explaining FRBs within our theory but, unless the two swarms are highly asymmetric, two transit windows separated by $120^\circ$ should be seen. However, given the small number of events, we simulated that two Trojan swarms with an orbital period of $3P$ could mimic an apparent period of $P$ as it would not be very different from an orbit with three equidistant swarms where the third one has been missed by (lack of) chance. Nonetheless, folding the FRB 180916.J0158+65 events at $3P$ should then show only two groups, and not three as it happens (see Fig. 1).

### 2.3. Hildas with period 2P

There exists another class of asteroids in the Solar system called the Hildas which does have the property of forming three equidistant swarms just inside the $L_3$, $L_4$ and $L_5$ points(Brož & Vokrouhlický 2008). These asteroids share an orbital period around the Sun of approximately 2/3 of that of Jupiter and have moderately eccentric orbits with $e \lesssim 0.3$ [2]. Hence, they undergo a 3:2 resonance with Jupiter such that their aphelia is successively near each of the three Lagrange point over three orbital periods. Contrary to the Trojans, they do not follow the Lagrange points but their stream accumulates near these points thus creating apparent swarms (Schubart 1991; Sharkey et al. 2016; Toth 2006) Three identical equidistant swarms (effectively) orbiting at $3P$ would be virtually impossible to distinguish from a single entity at $P$, unless the main companion's mass is sufficiently large such that the $L_3$ point be significantly closer to the pulsar than the two others, in which case the wind magnetic field would be larger at that point and create more intense, and therefore possibly more numerous, observable bursts. Another possibility, which we favour hereafter, is that both Hildas and Trojans co-exist in the system, thus making the population of asteroids denser along the line of sight of the observer at $L_4$ and $L_5$ than at $L_3$. In fact, it would seem rather arbitrary that only one type of asteroid exists and therefore more likely that both are present, if any. Note that bursts might also be created by the main companion, only is it very unlikely that our line of sight crosses its Alfvén wings in particular. If the orbital orientation was favourable one would see this particular burst repeating with a more accurate periodicity.

### 2.4. Burst statistics

Following the previous section, we assume for the remainder of this article that the 28 FRBs reported in (Collaboration et al. 2020) originate from three swarms of asteroids located at the $L3$, $L4$ and $L5$ Lagrange points of a companion orbiting a magnetized neutron star with a period $3P = 49.05$ days. We associate to each swarm a transit window of $\sim$ 4 days which has been observed in four daily 15min exposures (see also Fig. 2).

We note that bursts are usually not seen across all four exposure windows corresponding to a swarm transit. We call "visible exposure windows" those exposures during which at least one burst was recorded. Although in principle each individual burst could be due to a different asteroid, we have shown in MZV20 that it is likely that each asteroid results in several bursts bunched in a "wandering" time interval $\tau_w \sim$ 1h. This is due to the wandering motion of the source in the turbulent pulsar wind which results in the narrow beam sweeping a much wider area and possibly crossing several times the observer's line of sight. The extent of the area covered by the wandering beam translates into a characteristic wandering time during which the beam is susceptible to cross the line of sight, that is a burst remains possible. One can in principle infer $\tau_w$ from the bunching of observed bursts. Here, the small number of bursts together with the short, 15 min, contiguous observations makes any determination highly uncer-

[1] See the Trojan page of the Minor planet Center: `https://minorplanetcenter.net/db_search/show_by_orbit_type?utf8=%E2%9C%93&orbit_type=9`

[2] See Hildas at Minor Planet Centre: `https://minorplanetcenter.net/db_search/show_by_orbit_type?utf8=%E2%9C%9&orbit_type=8`

tain. However, we note that bunches of up to four bursts were observed in the same 15 min exposure window and that in seven transit windows out of eleven that contained bursts the totality of the bursts were observed during a single exposure (out of four per transit window), see Fig. 2. In addition, turbulence is expected to be only a small perturbation to the bulk radial motion of the wind, which implies that $\tau_w \ll 3P$. For these reasons, we assume that 1day $> \tau_w \gtrsim$ 15min and therefore that all the bursts occurring during a single 15 min exposure result from the transit of a single asteroid. In total 18 such transits were observed in Collaboration et al. (2020) (see Fig. 2). We also note that turbulence can explain the two pairs of bursts separated by only 60ms that were observed and which were, in this case, connected to the same object and not independent.

It readily appears that more than half of the swarm transit windows do not show any event (see Fig. 2). This may simply mean that no asteroid was transiting at all, consistent with the fact that often a single asteroid was seen during a transit window. However, it is also possible that an independent mechanism is making bursts visible only momentarily. The most likely mechanism is scintillation due to the interstellar/intergalactic medium. In most cases this causes an attenuation of the intrinsic flux of the source and more rarely enhances it (see e.g. Cordes & Chatterjee (2019)). Following Spitler et al. (2018), the refractive scintillation timescale is $\Delta t_r = 21,500 V^{-1} f^{-2.2}$ days, where $V \sim 1-10$ km.s$^{-1}$ is the motion of interstellar matter relatively to the Earth, and $f = 0.6$ Ghz is the frequency of the observed waves. Then $\Delta t_r \geq 6,000$ days; it does not correspond to the timescale characterizing the swarm transit windows, that are of the order of a few days. The diffractive scintillation has a faster timescale $\Delta_d = 15,000 V^{-1} f^{-1}$ seconds, ($V$ is still in km s$^{-1}$ and $f$ in GHz). In our case, $\Delta t_d = 1-8$ hours, consequently, diffractive scintillation can contribute to explain why some swarm transit windows contain bursts, and some others not.

Although the number of asteroid transits seen at each Lagrange point might be the result of a random fluctuation, or of a difference in the number of exposure windows not hidden by scintillation (see below), we assume for convenience in Fig. 1 and 2 that $L3$ corresponds to the smallest number of transits, 4, since it is the point where only Hilda asteroids can be seen. It follows that $L4$ contains the largest number of transits with a total of 9, and $L5$ had 5. We also note that $L3$ has the narrowest swarm transit duration as the bursts are distributed over 1 day, compared to 2 and 4 days for $L4$ and $L5$ respectively. This is correlated with the number of asteroids received from each swarm, but might also be indicative of their intrinsic sizes.

In this model, the properties of successive bursts, although generated by the same asteroid, should vary randomly from one burst to the next. The reason for this is that the intersection of the beam with the line of sight varies randomly. We verified that the normalised cross-correlation $c_x = \langle x_i x_{i+1} \rangle / \langle x_i \rangle \langle x_{i+1} \rangle$ is consistent with zero, where $x_i$ is a property $x$ of burst $i$ in a given visible exposure and the property can be either its fluence $F$, peak intensity $I$, or width $W$. We get $c_F = 0.1, c_I = 0.06, c_W = -0.1$. On the other hand, significant correlations would be expected if these bunches were related to an eruption-like mechanism, where aftershocks of lower intensity usually follow a primary event (see e.g. Aschwanden et al. (2016) for a discussion of this type of mechanism in the framework of self-organised criticality).

We have searched for asymmetries between the three Lagrange points that could reveal a $3P$-periodicity. In particular, we have performed pairwise two-sample Kolmogorov-Smirnov tests between the burst counts received at each Lagrange point (bottom panel of Fig. 1), thus trying to assert if these three samples derive from the same distribution. The results depend heavily on the number of exposures that are assumed hidden, for example by scintillation (see above), and are therefore inconclusive. Similarly, we have compared the three samples of width, peak intensity, and fluence (Fig. 1) and obtained inconclusive p-values ranging from 0.2 to 0.8. This illustrates the fact that unless there is a striking difference between the three swarms, the small sample sizes prevent any conclusion. In fact, we have checked by simulation that even if one swarm was missing altogether, a period of $P$ could still be favoured against a period of $3P$ in a periodogram such as the one reported in Collaboration et al. (2020). Indeed, due to the small sample, removing a swarm can be indistinguishable from a statistical fluctuation. Of course, in this case only two groups of bursts would appear on Fig 1.

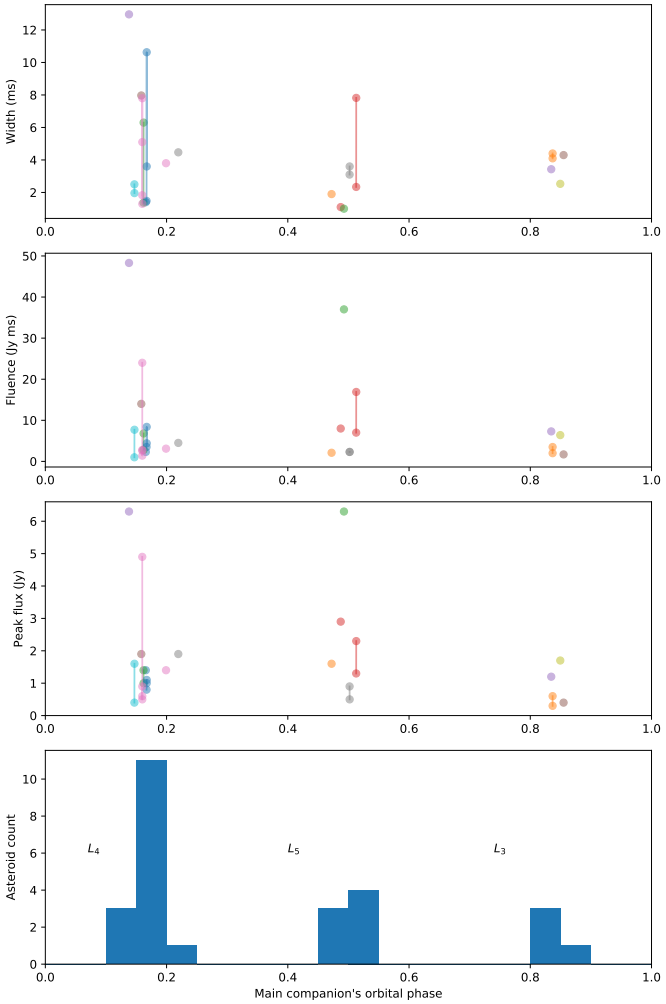


**Fig. 1.** Summary of the properties of the bursts of FRB 180916.J0158+65 as reported in Collaboration et al. (2020) as a function of the main companion's orbital phase, assuming an orbital period of $3P = 49.05$ days. Bursts associated to a single asteroid (and coincidentally to a single exposure window) have the same color and are connected to each other by a solid line when more than one burst was received. The bottom panel shows the number of independent events at each orbital phases i.e. pair of red circles in the above panels count for 1. The most probable Lagrange point associate with each group of bursts is indicated on the bottom panel.

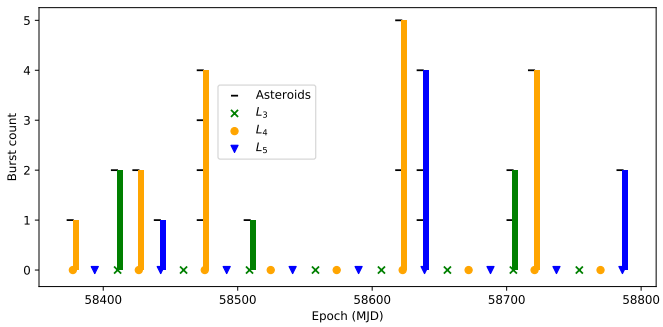


**Fig. 2.** Number of bursts seen during each swarm transit window in the time span of the observation reported in Collaboration et al. (2020). Each transit window lasts 4 days and was observed for $\sim$ 1h ($\sim$ 15min/day exposure) totalling $\sim$ 11h of exposure during transits on the entire observation span. Each black tick corresponds to one asteroid assuming a wandering time 15min $\lesssim \tau_w <$ 1d or, alternatively, to one visible exposure window.

### 2.5. Number of asteroids

Estimating the number of asteroids in the system requires further assumptions concerning the properties of the swarms. Following MZV20, we consider a simplistic model where the swarms cover an angle $\alpha = 0.1$rd in inclination, akin to the angle covered by the Trojans of the Solar system. The effective area covered by the emission beam is dominated by wandering in the turbulent pulsar wind, and we approximate it to a cone of aperture $\alpha_w \sim 2\pi\tau_w/P_{orb}$, and $P_{orb}$ is the orbital period. The visible asteroids are those contained within a band of thickness $\alpha_w$ in inclination. Assuming a uniform distribution of asteroids within three identical swarms one gets the total number of asteroids $3N_{swarm} = N_v\alpha/\alpha_w$, where $N_{swarm}$ is the number of asteroids in one swarm and $N_v$ is the number of visible asteroids during one orbital period. This relates to the average rate of transiting asteroids $n_a = N_v/P_{orb}$ such that

$$N_{swarm} = 1.2\times10^3\left(\frac{n_a}{4\mathrm{d}^{-1}}\right)\left(\frac{\alpha}{0.1\mathrm{rd}}\right)\left(\frac{P_{orb}}{49.05\mathrm{d}}\right)^2\left(\frac{\tau_w}{1\mathrm{h}}\right)^{-1}, \quad (1)$$

where we have estimated $n_a$ from 18 asteroids (see fig. 2) seen over 15 min of observation during 408 days. This rate could be somewhat higher if one assumed that a number of asteroids were missed due to scintillation. On the other hand, it is possible that some asteroids have been transiting several times, in which case this rate is overestimated. We have also used $P_{orb} = 3P$ which, although not the orbital period of Hilda asteroids, is the effective period over which the three swarms are transiting.

For comparison, the number of asteroids larger than 1km at the L4 Jupiter Trojan swarm is estimated to be $\sim 1.6\times10^5$ for a total mass of $\sim 10^{-4}M_{Earth}$ (Jewitt et al. 2000). Although the volume of dynamical stability of the swarms is not a straightforward problem (e.g. Levison et al. 1997) we note that the orbit of Jupiter is only $\sim$ 20 times wider than the orbit assumed here and therefore the density of asteroids does not need to be larger if the swarms span a similar angular size.

## 3. Pulsar and asteroid properties

A parametric study is conducted in order to see if the MZV20 model fits the characteristics of FRB 180916.J0158+65 when we set the companion orbital periods to $P$, $2P$ and $3P$. We tested various parameter sets with the same equations and the same constraints as in MZV20. Apart from the orbital periods $P_{orb}$ and the distance $D$ from the observer, the choice of the parameter set is the same as in MZV20, were it is discussed. Out of 1,336,500 parameters set tested for a pulsar, 140,382 of them could provide FRBs above 0.3 Jy, for companions (small or large) that do not evaporate, at a distance $D = 0.15$ Gpc from the observer (Marcote et al. 2020). When we restrict to asteroids of diameter $R_c < 10$ km, associated with a pulsar emitting more than $10^{27}$ W in the form of non thermal photons, with a spin-down age $\tau = P_*/\dot{P}_*$ larger than 10 years, we find 1,251 solutions. Details are given in appendix A. This study shows that FRB 180916.J0158+65 is compatible with young magnetized pulsars with short spin periods (3 or 10 ms), of ages $\tau = P/\dot{P}$ comprised between 10 years and a few centuries, surrounded by metal rich asteroids of size $R_c \leq 10$ km having orbital periods $P$, or $2P$ or $3P$. Those asteroids do not evaporate, therefore the duration of such systems as sources of FRBs is mainly constrained by the pulsar spin down, or said differently, by their spin-down age $\tau$. This mean that according to the present model, the repeating FRBs could be observed over a few decades of years and up to a few centuries with the present flux level.

## 4. Conclusion

We show in this article that the reported periodicity of FRB 180916.J0158+65 as well as properties in terms of peak flux and width can be explained by a relatively limited number of asteroids, a few thousands, immersed in a turbulent and magnetised wind of a young pulsar. Although the orbital configuration of the asteroid swarms that we suggest here, three dynamical Hilda-type swarms and two Trojan swarms following a main companion, has been shown to be stable in the Solar system, it is clear that further studies assessing both formation processes and stability are necessary.

From an observational point of view, if there is some evidence that asteroids could produce some of the observed pulsar timing noise Shannon et al. (2013), it is not known at present how frequent they are. However, our model presents the advantage of providing a number of falsifiable predictions which could be assessed within the next few years if observations remain as frequent as they have been in (Collaboration et al. 2020):

- The main periodicity will become $3P = 49.05$ days, corresponding to the orbital period of the main companion;
- One of the three groups of FRBs (when folded at $3P$) may become significantly smaller than the others;
- Rare bursts might be observed in between the three favoured orbital phases as Hilda asteroids can be at any orbital phase (only less likely outside of the Lagrange point regions).

Our study favours a very young pulsars, at most a few centuries old. We note that this is consistent with the apparent location of the source of FRB 180916.J0158+65 in a star-forming region of its host galaxy Marcote et al. (2020).

## Appendix A: Pulsar and companions characteristics compatible with FRB 180916.J0158+65

A parametric study is conducted in order to see if the mzv20 model fits the characteristics of FRB 180916.J0158+65 when we set the companion orbital periods to $P, 2P$ and $3P$. The model and notations are almost the same as in mzv20: a pulsar of 1.4 Solar mass, with a surface magnetic field $B_*$, a surface temperature $T_*$, a radius $R_*$ and a rotation period $P_*$, emits a power $\dot{E}_{\max}$ (also noted $(1-f)g\dot{E}_{\rm rp}$ in mzv20) in the form of high energy photons and wind kinetic energy, that contribute to the companion thermal balance. The power $\dot{E}_{\max}$ is less than the loss rate of rotational energy, because an important part of the rotational loss is in the form of the long-wavelength Poynting flux (Deutsch 1955) that is not absorbed by small companions (Kotera et al. 2016). The companion orbits at a distance $a$ ($r$ in mzv20) from the neutron star, where it is immersed in the pulsar wind of Lorentz factor $\gamma$. The companion is heated by the thermal radiation of the pulsar associated with $T_*$, by the high-energy photons and particles of the wind (both associated with $\dot{E}_{\max}$), and by the electric current induced by the Alfvén wings into the companion. This last contribution depends on its electrical conductivity $\sigma_c$, where $\sigma_c \sim 10^3$ for silicate rocks, and $\sigma_c \sim 10^7$ for an iron dominated body.

The radio emission power is proportional to the electromagnetic power associated with the Alfvén wing (Mottez & Heyvaerts 2011) with a yield coefficient $\epsilon$ (mz14, mzv20). In the reference frame of the radio source, that is the pulsar wind reference frame, we suppose that the waves are emitted within a solid angle $\Omega_A$. In the observer's frame, this solid angle is considerably reduced by the relativistic aberration. Regarding radio frequencies, the emission bandwidth is thought to be 1 GHz. The FRB duration $\tau$ is used in the computation of the source size (in our reference frame).

We consider a distance $D = 0.15$ Gpc between the source and the observer (Marcote et al. 2020). Since the detected pulses in Collaboration et al. (2020) have a flux $0.3 < S < 6.6$ Jy, we retain parameter sets corresponding to pulses exceeding 0.3 Jy from the distance $D = 0.15$ Gpc.

The procedure is the same as in mz20 : we try the 1336500 combinations of parameters displayed in Table A.1, that correspond to bodies orbiting pulsars with a high magnetic field. We then select the cases that meet the following conditions: (1) the observed signal amplitude on Earth must exceed 0.3 Jy; (2) the companion must be in solid state with no melting/evaporation happening; (3) the radius of the source must exceed the maximum local Larmor radius. This last condition is a condition of validity of the MHD equations that support the theory of Alfvén wings. Practically, the larger Larmor radius might be associated with electron and positrons. In our analysis, this radius is compiled for hydrogen ions at the speed of light, so condition (3) is checked conservatively.

Among those parameter sets, 140382 fit our conditions. Because we are interested in small companions and by fairly energetic pulsars, we then require $R_c \leq 10$ km, and $\dot{E}_{\max} \geq 10^{27}$ W, and a pulsar spin-down age $\tau = P_*/\dot{P}_* > 10$ years (see mzv20 for the evaluation of $\tau$ in our analysis). We then get 197 solutions for an orbital period $P_{\rm orb} = P$, 299 for Hildas companions ($P_{\rm orb} = 2P$) and 252 for Trojans ($P_{\rm orb} = 3P$). All of them exclude a period $P_*$ of 30 ms. Only 10 and 3 ms are retained. A few of them are detailed in Table A.2.

Let us consider the 299 solutions associated with Hildas companions with orbital period $2P$. By definition, they all correspond to a flux above 0.3 Jy, but 20 of them correspond to bursts above 10 Jy. All of them involve metal rich companions, with $\sigma_C \geq 100$ Mho. We find solutions with $R_c \leq 2$ km. The neutron star temperature does not constrains very much the solutions, and $T_* = 3.0E+06$ can be reached without problem. The smallest obtained wind Lorentz factor is $\gamma = 3.0E+05$. The smallest magnetic field $B_* = 3.2E+07$ T. The non-thermal radiations are more constraining : the largest found value is $\dot{E}_{\max} \geq 1.0E+28$ W. The spin-down age in years is comprised in the range $11.4 \leq \tau \leq 642.3$. Then, only young pulsars can be a cause of Hildas (or Trojans) FRB associated with FRB 180916.J0158+65 .

There are 252 solutions associated with Trojan companions with orbital period $3P$, and 12 of them correspond to bursts above 10 Jy. Their characteristics are very similar to those of Hildas with orbital period $2P$ ; they exhibit almost the same maximal and minimal figures.

We should mention here that the thermal constraints are computed for circular orbits. For Hildas, with a period $2P$ a corresponding semi-major axis $a = 0.22$ AU, and eccentricity $e \sim 0.3$ (in the Solar system $0 \leq e \leq 0.3$), the periastron distance is $r_p = 0.15$ is similar to the semi-major axis $a = 0.14$ corresponding to a circular orbit of period $P$. Therefore, the thermal constraints of Hildas are somewhere between the cases $P$ and $2P$ of Table A.2, and the constrains relative to the radio-emission power are those corresponding to a period $2P$.

In any case, we can see that FRBs caused by small companions ($R_c$ down to 2 km) are associated with a highly magnetized pulsar with periods about 3 or 10 ms. This class of pulsars is represented in our Galaxy by the Crab pulsar and more generally young pulsars.

*Acknowledgements.* G. Voisin acknowledges support of the European Research Council, under the European Union's Horizon 2020 research and innovation programme (grant agreement No. 715051; Spiders).

## References

Aschwanden, M. J., Crosby, N. B., Dimitropoulou, M., et al. 2016, Space Science Reviews, 198, 47
Brož, M. & Vokrouhlický, D. 2008, Monthly Notices of the Royal Astronomical Society, 390, 715
Collaboration, T. C., Amiri, M., Andersen, B. C., et al. 2020, arXiv:2001.10275 [astro-ph], arXiv: 2001.10275
Cordes, J. M. & Chatterjee, S. 2019, Annual Review of Astronomy and Astrophysics, 57, 417
de Pater, I., Gibbard, S. G., Chiang, E., et al. 2005, Icarus, 174, 263
Deutsch, A. J. 1955, Annales d'Astrophysique, 18, 1
Jewitt, D. C., Trujillo, C. A., & Luu, J. X. 2000, The Astronomical Journal, 120, 1140
Kotera, K., Mottez, F., Voisin, G., & Heyvaerts, J. 2016, Astronomy & Astrophysics, 592, A52
Levison, H. F., Shoemaker, E. M., & Shoemaker, C. S. 1997, Nature, 385, 42
Lyne, A. & Graham-Smith, F. 2012, Pulsar Astronomy, 4th edn. (Cambridge ; New York: Cambridge University Press)
Marcote, B., Nimmo, K., Hessels, J. W. T., et al. 2020, Nature, 577, 190
Michilli, D., Seymour, A., Hessels, J. W. T., et al. 2018, Nature, 553, 182
Mottez, F. & Heyvaerts, J. 2011, Astronomy and Astrophysics, 532, A21+
Mottez, F. & Zarka, P. 2014, Astronomy and Astrophysics, 569, A86
Neubauer, F. M. 1980, J. Geophys. Res., 85, 1171
Petroff, E., Hessels, J. W. T., & Lorimer, D. R. 2019, The Astronomy and Astrophysics Review, 27, 4
Schubart, J. 1991, Astronomy and Astrophysics, 241, 297
Shannon, R. M., Cordes, J. M., Metcalfe, T. S., et al. 2013, The Astrophysical Journal, 766, 5
Sharkey, B., Ryan, E. L., Woodward, C. E., & Noll, K. S. 2016, in American Astronomical Society Meeting Abstracts, Vol. 227, American Astronomical Society Meeting Abstracts #227, 141.10
Sicardy, B. & Lissauer, J. J. 1992, Advances in Space Research, 12, 81
Spitler, L. G., Herrmann, W., Bower, G. C., et al. 2018, ApJ, 863, 150
Toth, I. 2006, A&A, 448, 1191

**Table A.1.** Parameter set of the first parametric study of FRBs produced by pulsar companions of medium and small size. The last column is the number of values tested for each parameter. The total number of calculations is the product of all values in the last column, i.e. 217,728.

| Input parameters | Notation | Values | Unit | Number of val. |
|---|---|---|---|---|
| NS magnetic field | $B_*$ | $1.0E+073.2E+071.0E+083.2E+081.0E+09$ | T | 2 |
| NS radius | $R_*$ | $1.0E+011.1E+011.2E+011.3E+01$ | km | 2 |
| Rotation period | $P_*$ | $3.2E-031.0E-023.2E-021.0E-013.2E-01$ | s | 4 |
| NS temperature | $T_*$ | $3.0E+051.0E+063.0E+06$ | $10^5$ K | 3 |
| wind Lorentz factor | $\gamma$ | $1.0E+053.0E+051.0E+06$ | | 3 |
| radio efficiency | $\epsilon$ | $1.0E-02$ | | 2 |
| Companion orbital period | $P_{\rm orb}$ | $P, 2P, 3P$ | $P$ = 16.34 d | 3 |
| companion radius | $R_c$ | $1.0E+01\,2.2E+01\,4.6E+01\,1.0E+02$ | m | 7 |
| companion radius | $R_c$ | $3.2E+021.0E+033.2E+031.0E+04$ | m | 7 |
| Emission solid angle | $\Omega_A$ | $1.0E-011.0E+001.0E+01$ | sr | 3 |
| Power input | $\dot{E}_{\rm max}$ | $1.0E+273.0E+271.0E+283.0E+281.0E+29$ | W | 4 |
| Companion conductivity | $\sigma_c$ | $1.0E-031.0E+021.0E+07$ | Mho | 3 |
| Distance to observer | $D$ | 0.15 | Gpc | 1 |
| bandwidth | $\Delta f$ | $\max(1, f_{ce}/10)$ | GHz | 1 |
| FRB duration | $\tau$ | $5.\,10^{-3}$ | s | 1 |

**Table A.2.** Examples illustrating the results of the parametric studies in Tables A.1 for pulsars with small companions. In all case, the NS temperature $T_*$ = 10| K.

| Parameter | $B_*$ | $R_*$ | $P_*$ | $\gamma$ | $a$ | $R_c$ | $\dot{E}_{\rm max}$ | $\sigma_C$ | $S$ | $\tau$ |
|---|---|---|---|---|---|---|---|---|---|---|
| Unit | T | km | s | | AU | km | W | Mho | Jy | yr |
| long $\tau$ | $3E+07$ | 10 | 0.003 | $1.0E+06$ | 0.141 | 10 | $3E+27$ | $1.0E+07$ | 0.5 | 1137.9 |
| large $S$ | $3E+08$ | 10 | 0.003 | $1.0E+06$ | 0.141 | 10 | $3E+27$ | $1.0E+07$ | 53.6 | 11.4 |
| long $P_*$ | $3E+08$ | 12 | 0.010 | $1.0E+06$ | 0.141 | 10 | $3E+27$ | $1.0E+07$ | 1.6 | 38.1 |
| low $\gamma$ | $1E+08$ | 11 | 0.003 | $3.0E+05$ | 0.224 | 10 | $3E+27$ | $1.0E+07$ | 0.3 | 64.2 |
| large $\tau$ | $3E+07$ | 11 | 0.003 | $1.0E+06$ | 0.224 | 10 | $1E+28$ | $1.0E+07$ | 0.4 | 642.3 |
| large $S$ | $3E+08$ | 10 | 0.003 | $1.0E+06$ | 0.224 | 10 | $1E+28$ | $1.0E+02$ | 21.3 | 11.4 |
| small $R_c$ | $3E+08$ | 10 | 0.003 | $1.0E+06$ | 0.224 | 2 | $1E+27$ | $1.0E+07$ | 1.0 | 11.4 |
| longer $P_*$ | $1E+09$ | 10 | 0.010 | $1.0E+06$ | 0.224 | 10 | $1E+27$ | $1.0E+02$ | 2.1 | 11.4 |
| longer $P_*$ | $3E+08$ | 11 | 0.010 | $1.0E+06$ | 0.224 | 10 | $1E+27$ | $1.0E+02$ | 0.4 | 64.2 |
| low $\gamma$ | $1E+08$ | 12 | 0.003 | $3.0E+05$ | 0.293 | 10 | $1E+28$ | $1.0E+02$ | 0.3 | 38.1 |
| low $\gamma$ | $3E+08$ | 10 | 0.003 | $3.0E+05$ | 0.293 | 10 | $1E+27$ | $1.0E+07$ | 1.1 | 11.4 |
| large $\tau$ | $3E+07$ | 12 | 0.003 | $1.0E+06$ | 0.293 | 10 | $1E+28$ | $1.0E+02$ | 0.4 | 381.1 |
| large $S$ | $3E+08$ | 10 | 0.003 | $1.0E+06$ | 0.293 | 10 | $1E+28$ | $1.0E+02$ | 12.4 | 11.4 |
| small $R_c$ | $3E+08$ | 10 | 0.003 | $1.0E+06$ | 0.293 | 2 | $1E+27$ | $1.0E+07$ | 0.6 | 11.4 |